



Improvements of Models in National Seismic Hazard Maps for Japan

N. Morikawa⁽¹⁾, H. Fujiwara⁽²⁾, J. Miyakoshi⁽³⁾

⁽¹⁾ Chief Researcher, National Research Institute for Earth Science and Disaster Resilience, morikawa@bosai.go.jp

⁽²⁾ Director, National Research Institute for Earth Science and Disaster Resilience, fujiwara@bosai.go.jp

⁽³⁾ General Manager, Ohsaki Research Institute, Inc., miya@ohsaki.co.jp

Abstract

The seismic activity model for National Seismic Hazard Maps for Japan (NSHMJ) was significantly improved in 2014 based on the lessons from the 2011 great Tohoku earthquake, but we have continued to study further model improvements. For the large-to-mega interplate earthquakes along the Japan trench and Kuril trench, we model them in consideration of the diversity of the source region based on the revised evaluations by Headquarters for Earthquake Research Promotion of Japan. For earthquakes occurring in major active fault zones, we revise the model of occurrence probability in which multiple segments are active simultaneously. In addition, we modeled earthquakes whose magnitude is less than 6.8 occurring in major active fault zones, and change the top depth of source fault model from several kilometers to 0km based on the knowledges from the 2016 Kumamoto earthquakes. As for the background earthquake model, we separate the crustal earthquakes from subduction earthquakes in the Pacific Ocean region. In addition, we introduce the latest subducting plate shape model, and re-estimate the ratio of the number of interplate and intraplate earthquakes considering their focal mechanism solution. We model the frequency-magnitude distribution based on the earthquake catalogue including events after the 2011 great Tohoku earthquake, taking into account epistemic uncertainty. On the other hand, modeling of active faults in the sea region remains as a future issue.

In order to promote the engineering use of NSHMJ, we estimate the seismic hazard assessment of the response spectrum. In this study, we apply three ground motion prediction equations (GMPEs). We find that the results show large differences depending on the GMPE. The difference is greatly influenced by the ground motion prediction results with extremely few records such as mega-earthquakes or near-source region. However, one of the most important factors causing such a large difference is that individual database have been built for each Japanese GMPE, and the definition of ground motion index and processing procedures of waveform records have been not unified.

Also we have started to provide the hazard curve data on the web site, which is separately disassembled for earthquakes occurring in major active fault zones and major subduction earthquakes.

Keywords: National Seismic Hazard Maps for Japan; active faults; subduction earthquakes; seismic activity model; ground motion prediction equation



1. Introduction

After the 1995 Hyogo-ken Nanbu (Kobe) earthquake, preparation of the National Seismic Hazard Maps for Japan (NSHMJ) was initiated. The first version of the NSHMJ, consisting of probabilistic seismic hazard maps and scenario earthquake shaking maps, was published in 2005 by the Earthquake Research Committee, Headquarters for Earthquake Research Promotion of Japan (HERP), with annual updates through 2010, including a major revision in 2009. Furthermore, the seismic activity model for NSHMJ was significantly improved in 2014 based on the lessons from the 2011 great Tohoku earthquake.

However, further model improvements have continued to be studied based on the newly published evaluations of earthquakes by HERP and new insights from recent earthquakes. Ways to further utilize the NSHMJ have also been investigated, and these efforts are outlined in this work.

2. Improvements of seismic activity model

2.1 Subduction earthquakes

2.1.1 Earthquakes along the Kuril Trench

An evaluation of occurrence potentials of subduction-zone earthquakes along the Kuril Trench was published in December 2017 by HERP [1]. Based on the evaluation, the fault models of a mega-earthquake and interplate huge earthquakes in Tokachi-oki and Nemuro-oki were updated. In the conventional model, only one fault model was set for each earthquake. In the new model, various fault models were constructed for each earthquake considering that the earthquake magnitude was evaluated in a wide range by HERP. As a result, 13, 34, and 24 fault models were set for the mega-earthquake (Mj8.7–9.2), Tokachi-oki earthquake (Mj8.0–8.6), and Nemuro-oki earthquake (Mj8.0–8.5), respectively. Here, “Mj” is the Japan Meteorological Agency (JMA) magnitude. Fig. 1 shows fault models for the mega-earthquake as an example.

The occurrence probability of each earthquake was evaluated by using a Brownian passage time distribution model. The seismic hazard was assessed assuming that an earthquake occurred in one of the many fault models. Weighting was performed to follow the Gutenberg–Richter relation with a b-value of 0.9, and a model with a small-scale earthquake was more likely to occur (Fig. 2). When multiple fault models were included for an earthquake of the same magnitude, the weights were equally distributed for each fault model.

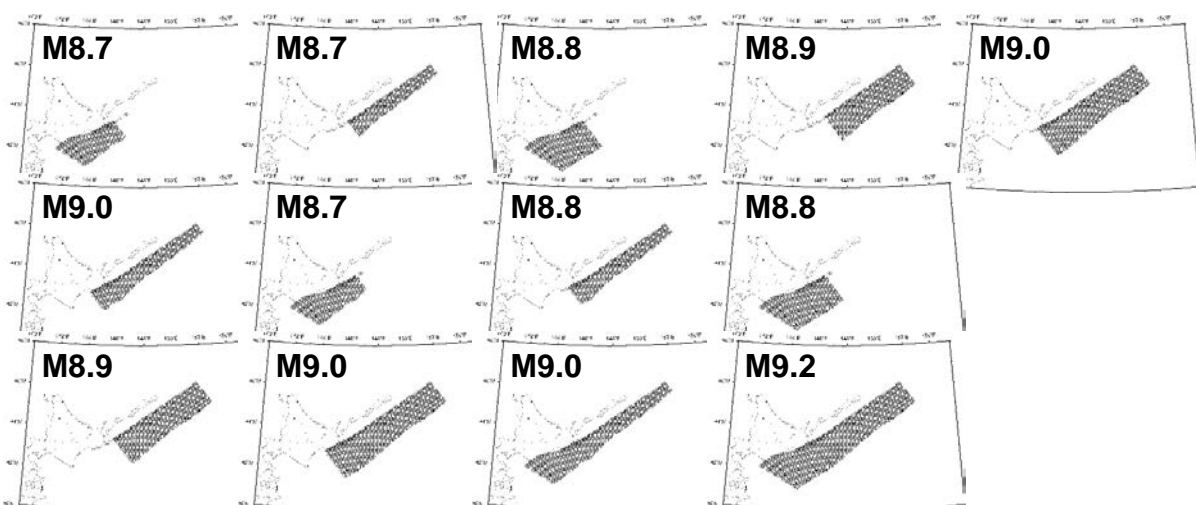


Fig. 1 – Fault models of mega-earthquakes along the Kuril Trench



2.1.2 Earthquakes along the Japan Trench

The evaluation of occurrence potentials of subduction-zone earthquakes along the Kuril Trench was published in February 2019 by HERP [2]. Based on the evaluation, the fault models of the 2011 Tohoku-type mega-earthquake and interplate huge earthquakes in Aomori-oki and Miyagi-oki were updated. Various fault models were constructed, as for the earthquakes along the Kuril Trench. Finally, 10, 51, and 20 fault models were set for the 2011 Tohoku-type earthquake (Mj8.6–9.0), Aomori-oki earthquake (Mj7.9–8.8), and Miyagi-oki earthquake (Mj7.9–8.6), respectively.

The occurrence probability was also evaluated for each earthquake. However, the Miyagi-oki earthquake was evaluated using the Poisson model. Weighting was performed as for the Kuril Trench. However, the huge interplate earthquakes in Aomori-oki and Miyagi-oki are not known to have been preceded by larger earthquakes in the past. Therefore, the weight was set to 1/50 for the Aomori-oki earthquake of Mj8.4 or more and for the Miyagi-oki earthquake of Mj8.3 or more (Fig. 2).

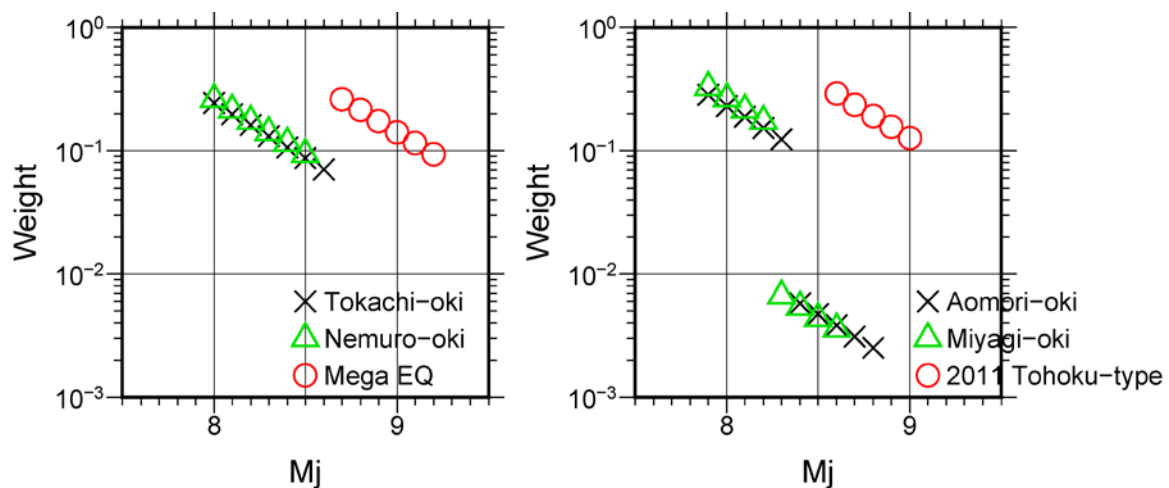


Fig. 2 – Weights of occurrence probability for earthquakes along the Kuril Trench and the Japan Trench

2.2 Earthquakes occurring in major active faults

2.2.1 Occurrence probability of earthquakes in which multiple segments are active simultaneously

In evaluations of earthquakes in the major active fault zones by HERP, it is stated that there is a possibility of an earthquake in which multiple segments are active simultaneously, but its occurrence probability is unknown. However, the probability of an earthquake occurring in each single segment has been evaluated by HERP. In this study, the occurrence probability is divided according to the following procedure.

- 1) Assign a half of the occurrence probability to earthquakes that occur in a single segment first.
- 2) For the segment with the lowest occurrence probability, the remaining half of the occurrence probability is equally divided into earthquake patterns due to simultaneous activity of multiple segments, including that segment.
- 3) Divide similarly in the order of the segment with the lowest occurrence probability.

This model was set up with reference to the concept of the Working Group on California Earthquake Probabilities [3].

2.2.2 Earthquakes smaller than Mj6.8

Earthquakes smaller than Mj6.8 that recently occurred in the major active fault zones caused damage near the source fault. In the current seismic activity model, not only the “characteristic earthquake” with magnitude M_c but also “earthquakes with hardly recognized surface traces” whose magnitude is between 6.8



and M_c are included. However, earthquakes smaller than $M_j6.8$ are modeled as background earthquakes without specified source faults. The occurrence frequency of the earthquakes with hardly recognized surface traces is modeled by distributing half the frequency of the characteristic earthquakes according to the Gutenberg–Richter relation. In this study, the occurrence frequency was extrapolated to $M_j6.5$, as shown in Fig. 3. The characteristic earthquakes are separately modeled. Fig. 4 shows the comparison of results of seismic hazard assessment between the current NSHMJ model and the model suggested in this study. It was confirmed that the $M_j6.5$ – 6.7 earthquakes in major active fault zones have increased the level of seismic hazard in the region near the major active fault zones.

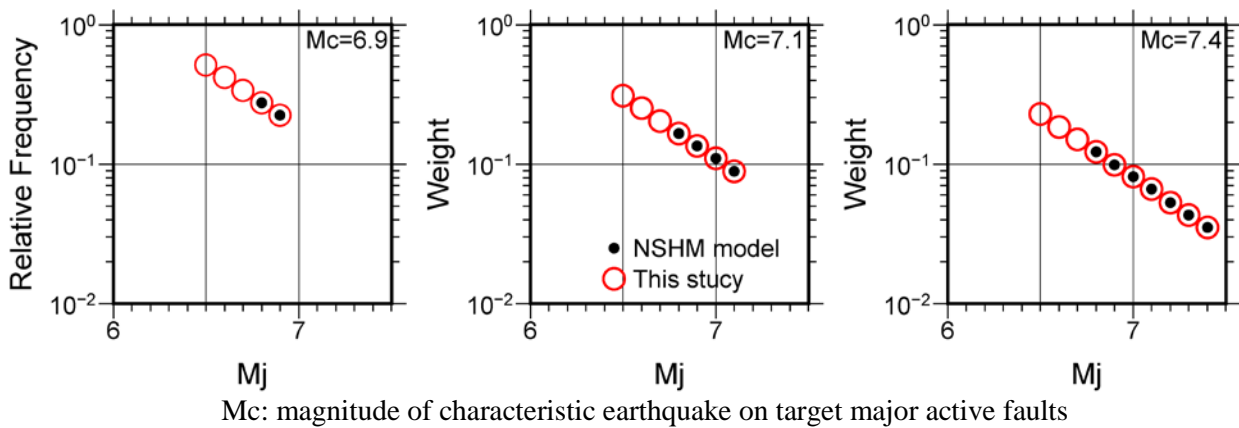


Fig. 3 –Relative occurrence frequency of earthquakes including $M_j6.5$ – 6.7 that occur on major active faults.

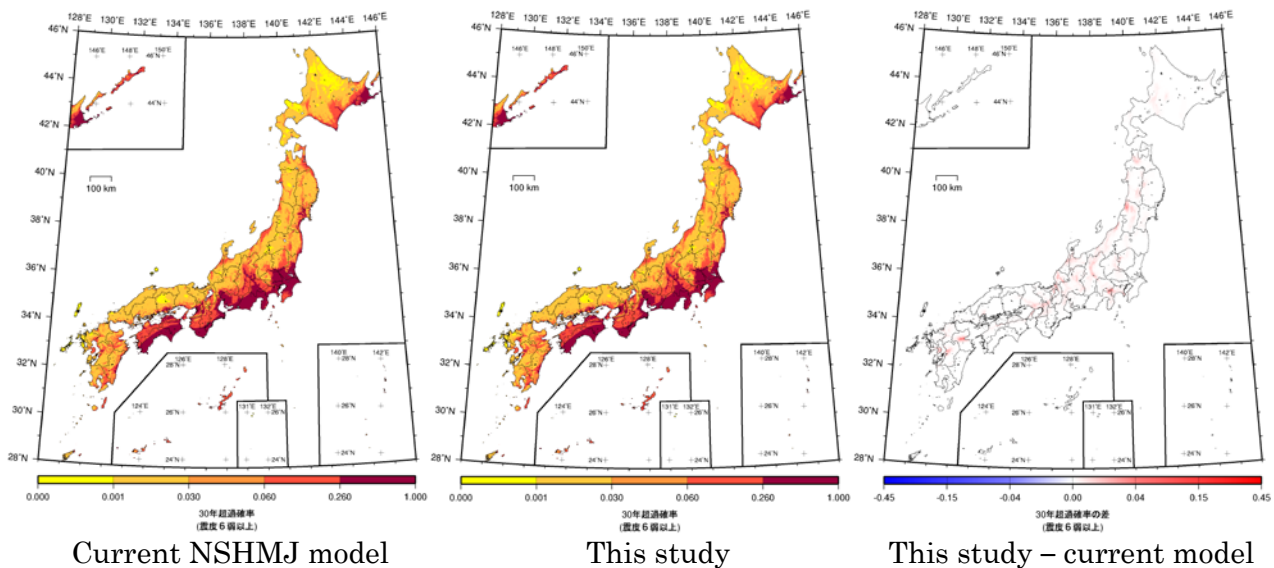


Fig. 4 – Comparison of seismic hazard assessment results between the current NSHMJ model and model including $M_j6.5$ – 6.7 earthquakes on active faults (distribution of exceedance probability of JMA seismic intensity ≥ 6 -lower within 30 years)

2.2.3 Top depth of the fault model

In the current NSHMJ model in Japan, the top depth of the fault model of the major active fault zones has been set to a basement of seismic bedrock, whose shear-wave velocity (V_s) is approximately 3000 m/s



instead of the ground surface of 0 km. This model results from the idea that relatively short-period ground motion with a period of several seconds or shorter, which is the main target period of the ground-motion evaluation in NSHMJ, has not been released from faults shallower than the seismic bedrock. However, large-amplitude strong-motion records with a dominant period of several seconds and permanent displacement were obtained during the main shock of the 2016 Kumamoto earthquake (Mj7.3). It is now recognized that ground motion, including permanent displacement, needs to be considered in the seismic hazard assessments in Japan.

Fig. 5 shows a comparison of the results between the current NSHMJ model and the model in which the top depth of the fault models set to 0 km. The level of seismic hazard near the surface trace of the active faults becomes larger than in the current model. The difference is remarkable near the major active fault zones in and around the large basin with thick sediments.

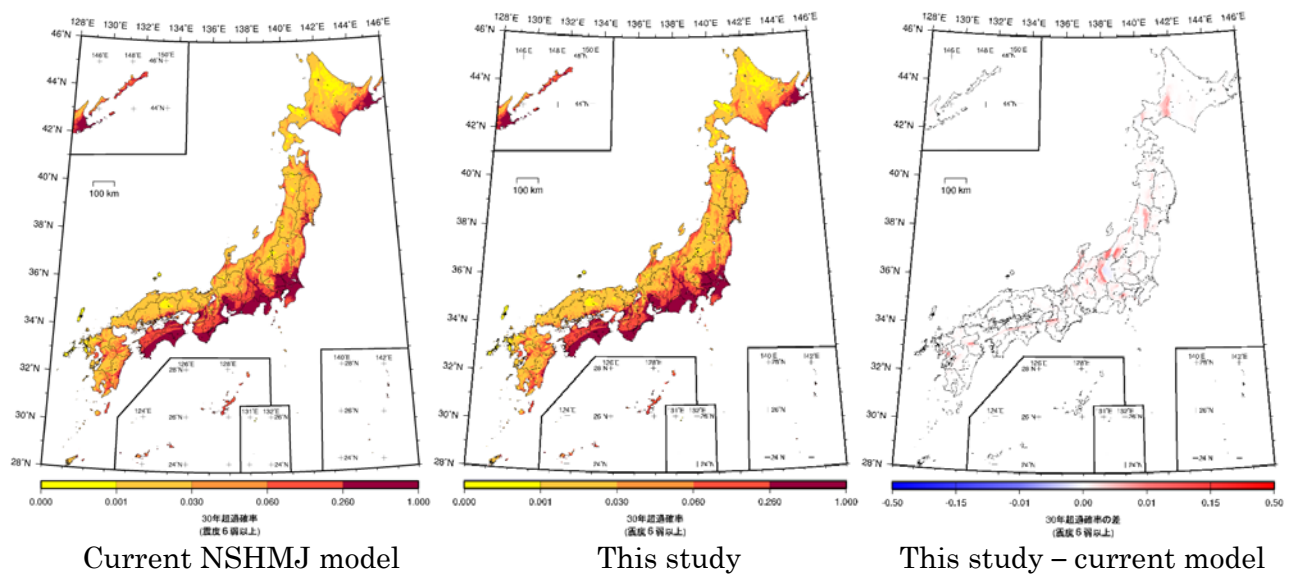


Fig. 5 – Comparison of seismic hazard assessment results between the current NSHMJ model and the model that top depth of fault models set to 0km

2.3 Background earthquakes

2.3.1 Revisions of zonings

The focal depth of the 2019 Hokkaido Eastern Iwate earthquake (Mj6.7) was approximately 40 km. In the source region, only the crustal earthquakes with a depth of less than 25 km and intraslab earthquakes with a depth of more than 100 km are modeled in the current NSHMJ. The off-Fukushima earthquake in November 2016 (Mj7.5) was a crustal earthquake that occurred in the region where only the subduction earthquakes are modeled in the current NSHMJ. In addition, the zonings in the evaluation of subduction earthquakes by HERP described in Section 2.1 have been changed since then. Based on these facts, the zoning of background earthquakes was revised.

Earthquakes at a depth of 25–45 km have already been considered in the current NSHMJ model, as the Urakawa-oki earthquakes in zone No. 1 in Fig. 6(a). The No. 2 zone, which is the source region of the 2019 earthquake, was added. Furthermore, the seismic activity at the same depth was carefully investigated, the shape of the No. 1 zone changed slightly, and zone No. 3 was also added. This model was proposed by HERP's Secretariat. Regarding the crustal earthquakes in the Pacific Ocean area, the zones shown in Nos.



30–36 in Fig. 6(b) were added. In accordance with this, the seaside boundaries of Nos. 7 and 9 were slightly changed to be near the coastline.

For subduction earthquakes, some zonings have been revised based on the evaluations by HERP described in Section 2.1 [1, 2], as shown in Fig. 6(c). Furthermore, regarding earthquakes in the Philippine Sea Plate, two new zones outside the trench axis, shown in Nos. 8 and 9 in Fig. 6(d), have been added, as were those in the Pacific Plate.

In the model of background earthquakes in NSHMJ, both a zoning method, as shown in Fig. 6, and Frankel's [5] non-zoning method are used. As with the current NSHMJ, zoning and the non-zoning methods have the equal weight.

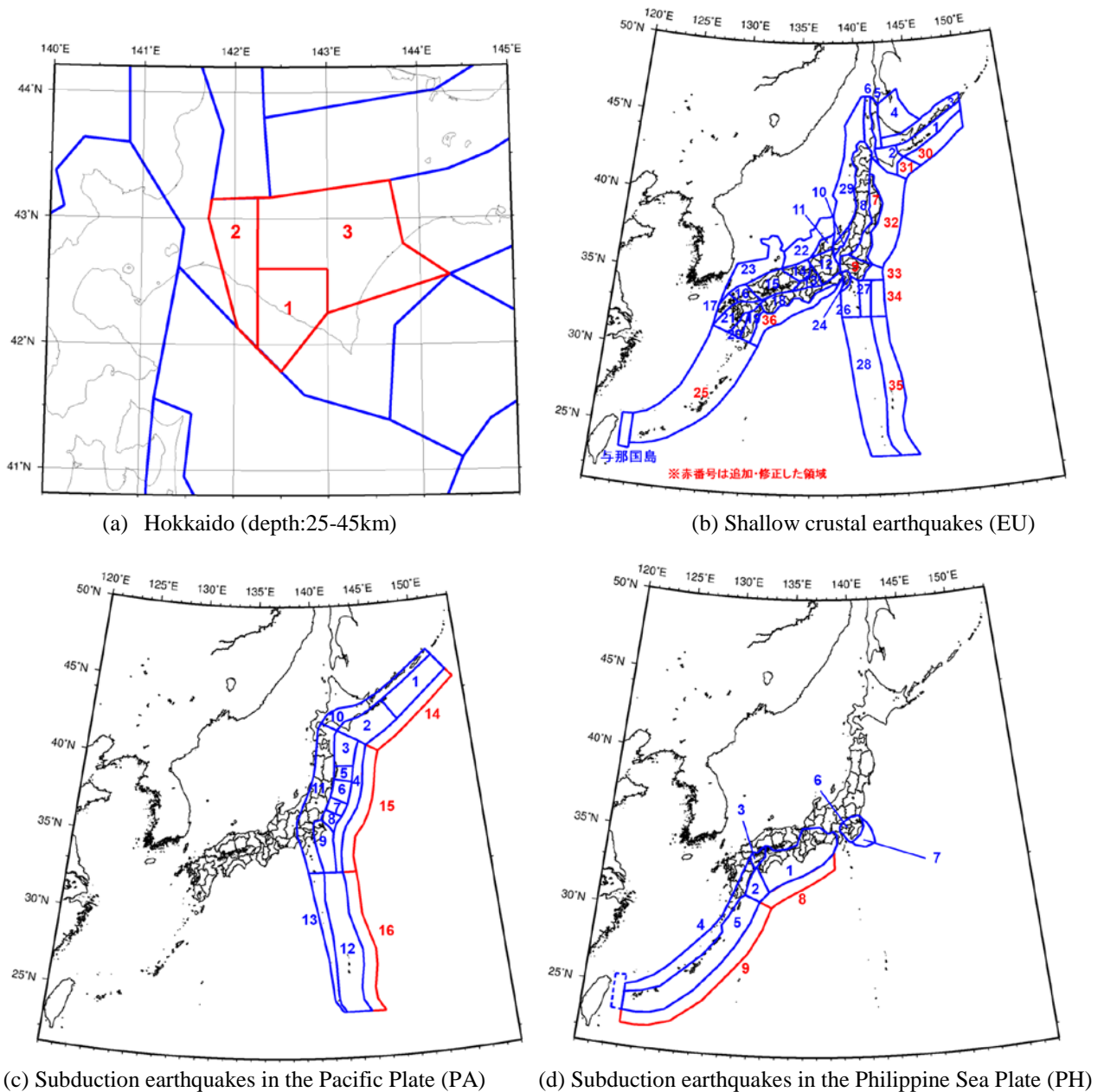


Fig. 6 – New zonings of background earthquakes added or changed in this study (red numbers)



2.3.2 Earthquake catalog after the 2011 great Tohoku earthquake

Earthquakes that occur 90 days from the occurrence of an earthquake of Mj6.0 or more have been removed from the earthquake catalog in the current NSHMJ model as aftershocks. However, one cannot apply the same rule to remove aftershocks of the 2011 great Tohoku earthquake, because many aftershocks and induced earthquakes occurred in and around the source region after the great earthquake. Therefore, the earthquake catalog until the end of 2010 is used in the current NSHMJ model. The seismic activity in the source region of the 2011 great earthquake attenuated rapidly until approximately three years after the event and gradually decreased. However, the activity level remained approximately 1.5 times higher than the level before the event as of March 2019 [6]. In this study, the earthquake catalog from 2011 to 2017 by the JMA[7] was added in the new model. Two catalogs were prepared in this study to address the uncertainty of seismic activity after the 2011 great earthquake. One had the aftershocks removed, the same as in the current model, and earthquakes that occurred in the source region of the 2011 great earthquake during the three years after the earthquake were removed from the catalog as aftershocks. The other is a catalog that includes all earthquakes — that is, a catalog that does not remove aftershocks. The new catalogs consist of earthquakes of Mj6.0 or more from 1885 to 1921 by Utsu [8] and earthquakes of Mj5.0 or more from 1922 to 2017 by JMA [7]. Fig. 7 shows a comparison of the cumulative annual frequency distributions in the two earthquake catalogs. The frequency in the catalog containing all earthquakes is two to three times larger than that of the catalog in which aftershocks in the source region of the 2003 Tokachi-oki (PA02) and the 2011 great Tohoku (PA05) earthquakes were removed. Similar trends can be seen in zones of crustal earthquakes next to the source region of the 2011 great earthquake (UE07, EU09).

2.3.3 New subducting plate model

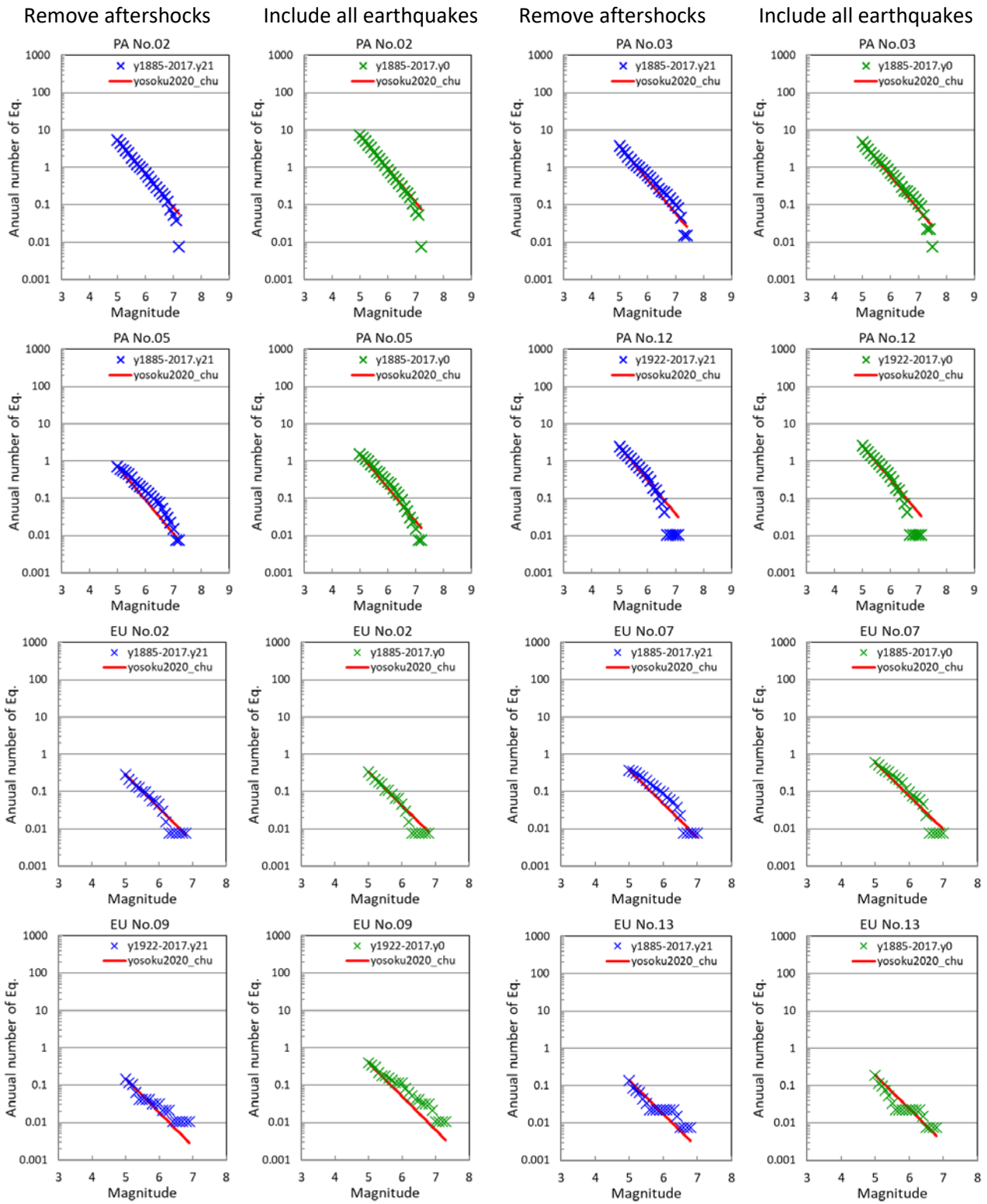
HERP updated the model of subducting plate shape in the evaluations for subduction earthquakes described in Section 2.1 [1, 2]. The fault models constructed in Section 2.1 were set according to the new plate shape. In addition, the focal depth of background earthquakes was also adjusted to the new plate shape.

The ratios of the numbers of interplate and intraplate earthquakes have been determined based on the hypocenter locations using the previous plate shape modeled. In this study, an attempt was made to determine the ratio considering not only the hypocenter location but also the fault mechanism solution by F-net [9]. The Kagan angle [10] was calculated based on the shape, direction of the plate motion evaluated by HERP, and fault mechanism solution. Table 1 shows the ratio of the number of interplate earthquakes in the Pacific Ocean Plate in the case in which the earthquakes with a Kagan angle within 30° were assumed to be interplate earthquakes. The ratio of the number of interplate earthquakes is smaller than in the current NSHMJ model, because there were quite a few non-thrust earthquakes, even though their hypocenters were located near the plate boundary. Here, only the separation of interplate and intraplate earthquakes was considered. However, shallow crustal earthquakes need to be separated from them further, as described in Section 2.3.1. This is an issue for the future.

3. Seismic hazard assessment of response spectrum

3.1 Selection of ground motion prediction equations (GMPEs)

Although peak velocity and JMA seismic intensity are used as ground-motion parameters in NSHMJ, the seismic hazard assessment using the response spectrum is useful for engineering use. However, many strong-motion records have been obtained by strong-motion observation networks, which were established after the 1995 Kobe Earthquake. As a result, many researchers have proposed ground-motion prediction equations for Japan. In this study, from the viewpoint of application to seismic hazard assessment for the whole of Japan, GMPEs that satisfy the following conditions were selected: 1) models that can be evaluated for each earthquake type, such as crustal, subduction interplate, and intraslab earthquakes, 2) models that can be evaluated for anomalous seismic intensity distributions during subduction earthquakes, 3) models applicable to magnitude 9 class earthquakes, and 4) models that can be evaluated on engineering bedrock with a Vs30



*Red line: current NSHMJ model

Fig. 7 – Comparison example of cumulative occurrence frequency in two earthquake catalogs (see Fig.6 for zone numbers)



Table 1 – Ratio of number of inter-plate earthquakes in the Pacific Plate (see Fig.6 for zone numbers)

Zone number.	3	5	6	7	8	9
Current NSHMJ model	0.952	0.952	0.952	0.952	0.889	0.889
This study	0.727	0.400	0.594	0.559	0.519	0.497

of 400 m/s. The GMPEs of Morikawa and Fujiwara (2013) [11] and Zhao et al. (2016) [12–14] satisfy all the above conditions. However, strong-motion records of magnitude 9 class earthquakes consist of those from the 2011 great Tohoku earthquake only. Therefore, one more GMPE, that of Goda and Atkinson [15] that satisfies the other three conditions was added to consider the uncertainties in the application of strong-motion prediction to the Nankai Trough earthquake.

3.2 Comparison of GMPEs and calculated uniform hazard spectrum

Fig. 8 shows a comparison of 5%-damped acceleration response spectra predicted by the three selected GMPEs. In the figure, the average shear wave velocity up to a 30-m depth (V_{s30}) is assumed to be 400 m/s for two GMPEs [11, 15] and the site class I for Zhao's GMPE [12–14]. The amplification by deep sedimentary layers modeled by Morikawa and Fujiwara's GMPE [11] is not considered in the figure. Regarding Goda and Atkinson's GMPE [15], an equation for shallower earthquakes was applied to crustal and interplate earthquakes, and an equation for deeper earthquakes was applied to intraplate earthquakes. The results show large differences, depending on the GMPE. The differences are greatly influenced by the ground-motion prediction results with extremely few records, such as mega-earthquakes or near-source regions.

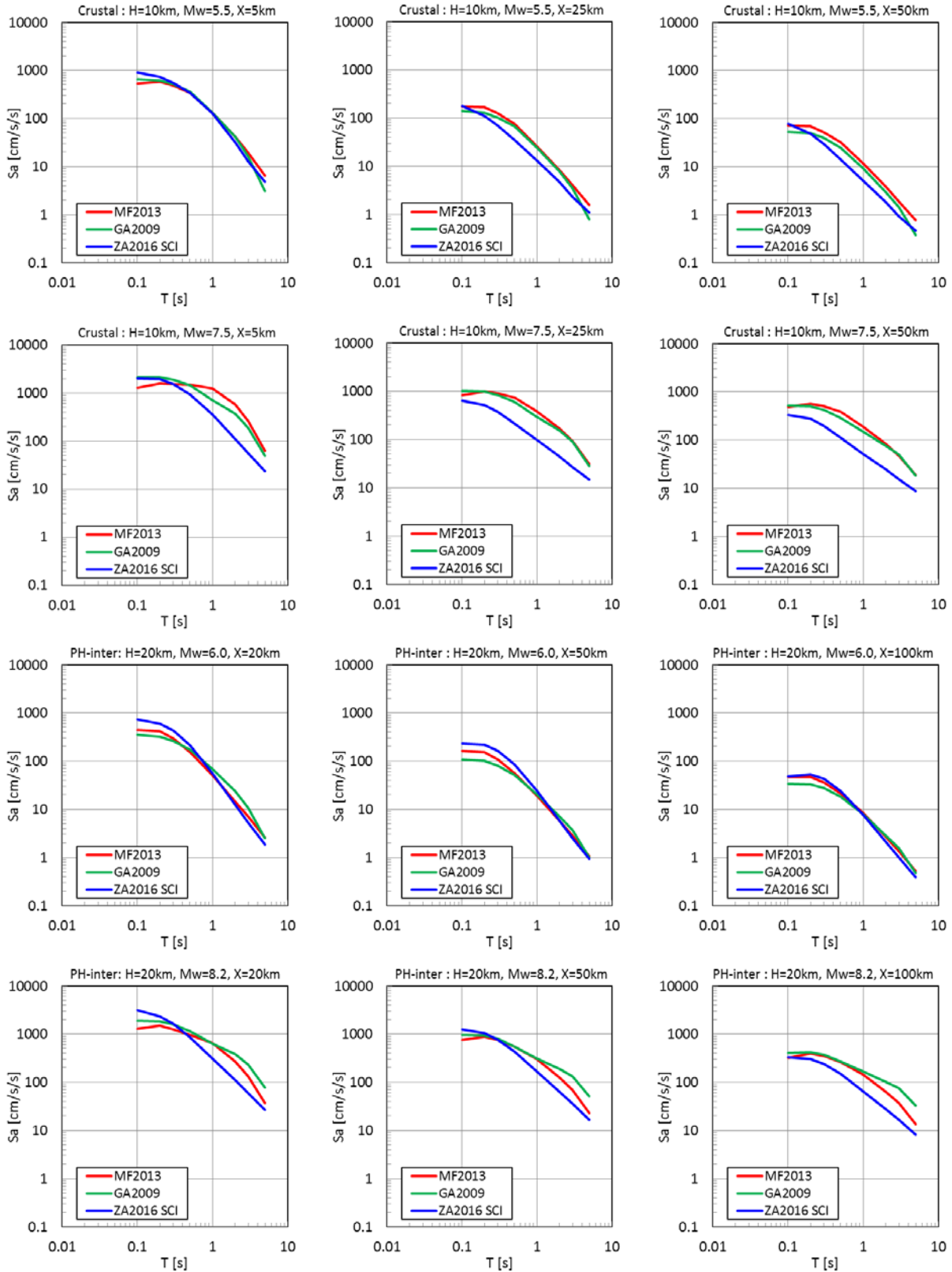
Fig. 9 shows an example of calculated uniform hazard spectra on the engineering bedrock using the three selected GMPEs. The seismic activity model of NSHMJ, 2018 version [16], was used in the calculations. The influence of subduction earthquakes is large at the Tokyo (35.69N, 139.69E) site. However, the Uemachi fault zone, one of the major active fault zones in Japan, with a relatively high occurrence probability, is located nearby at the Osaka (34.69N, 135.50E) site. One can see remarkable differences among the uniform hazard spectra of the three GMPEs in low-probability regions, such as 2% within 50 years, and a short-period (approximately 0.1 s) ground-motion range.

4. Detailed disaggregation of hazard curve for earthquakes in active fault zones

Hazard curve data of NSHMJ in each 250-m square mesh can be viewed and downloaded through the web system, Japan Seismic Hazard Information Station (J-SHIS) [17]. Until the 2016 version of NSHMJ, the hazard curves of earthquakes that occurred on active fault zones in each 250-m mesh were integrated into one. Here, we started to provide the data disaggregated into the hazard curves of earthquakes by individual active fault zones from the 2017 version of NSHMJ. This is expected to utilize NSHMJ further, such as in seismic risk assessment.

5. Conclusions

The improvements of the seismic activity model in NSHMJ were described, and the seismic hazard assessment of the response spectrum and detailed disaggregation of hazard curves for further use of NSHMJ were performed. The new models regarding subduction earthquakes along the Kuril Trench, described in Section 2.1.1, and occurrence probability of earthquakes in which multiple segments are active simultaneously, described in Section 2.2.1, have already been applied to the published NSHMJ. The new models regarding subduction earthquakes along the Japan Trench, described in Section 2.1.2, and background earthquakes, described in Sections 2.3.1 and 2.3.2, will be applied to the next version of NSHMJ. However, some models described in Sections 2.2.2, 2.2.3, and 2.3.3 require further study.



H: Focal depth, X: Fault distance

Red: Morikawa and Fujiwara (2013), blue: Zhao et al. (2016), green: Goda and Atkinson (2009)

Fig. 8 – Comparison of three ground motion prediction equations used in this study

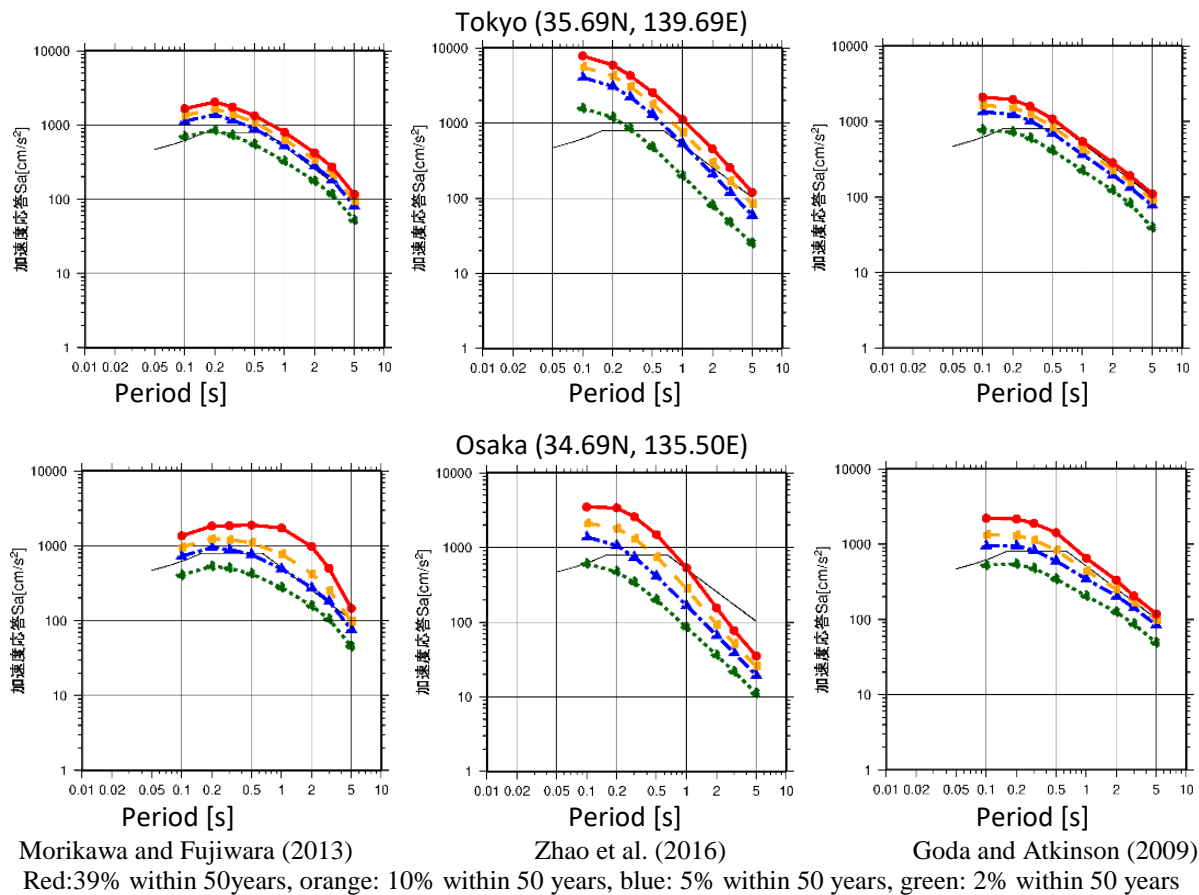


Fig. 9 – Examples of uniform hazard spectrum evaluated by three ground motion prediction equations.

Many strong motion records have been obtained since the 1995 Kobe earthquake, and several researchers have proposed GMPEs in Japan. However, individual databases have been built for each Japanese GMPE, and the definition of the ground-motion index and processing procedures of waveform records have been not unified. This situation causes the used ground-motion index and source and site parameters not to be unified among the databases. This makes it difficult to evaluate the validity or performance of GMPEs. As a result, it is difficult to select the optimal GMPE for the purpose of seismic hazard assessment. It is necessary to construct a “unified strong-motion database” in Japan.

6. Acknowledgements

This study has been carried out under the guidance of the Earthquake Research Committee, Headquarters for Earthquake Research Promotion of Japan, and relevant subcommittees. This study is being conducted as a part of the research project on “Research on Evaluation of Hazard and Risk” of the National Research Institute for Earth Science and Disaster Resilience.

7. References

- [1] Earthquake Research Committee, Headquarters for Earthquake Research Promotion (2017): Evaluation of occurrence potentials or subduction-zone earthquakes along the Kuril Trench (third edition). https://www.jishin.go.jp/main/chousa/kaikou_pdf/chishima3.pdf (in Japanese).



- [2] Earthquake Research Committee, Headquarters for Earthquake Research Promotion (2019): Evaluation of occurrence potentials or subduction-zone earthquakes along the Japan Trench. https://www.jishin.go.jp/main/chousa/kaikou_pdf/japan_trench.pdf (in Japanese).
- [3] Working Group on California Earthquake Probabilities (1995): Seismic hazards in southern California: Probable earthquakes, 1994 to 2024. *Bulletin of the Seismological Society of America*, **85**, 379-439.
- [4] Earthquake Research Committee, Headquarters for Earthquake Research Promotion (2016): Evaluation of Seismic Activities for November 2016. <https://www.jishin.go.jp/main/index-e.html>.
- [5] Frankel A (1995): Mapping Seismic Hazard in the Central and Eastern United States. *Seismological Research Letters*, **66** (4), 8-21.
- [6] Earthquake Research Committee, Headquarters for Earthquake Research Promotion (2019): Evaluation of Seismic Activities after “the 2011 off the Pacific Coast of Tohoku Earthquake”. <https://www.jishin.go.jp/main/index-e.html>.
- [7] Japan Meteorological Agency (2019): The Seismological Bulletin of Japan, Hypocenters. http://www.data.jma.go.jp/svd/eqev/data/bulletin/hypo_e.html.
- [8] Utsu T (1985): Catalog of large earthquakes in the region of Japan from 1885 through 1980 [Revision and addition], *Bulletin of the Earthquake Research Institute, University of Tokyo*, **60**, 639-642 (in Japanese with English abstract).
- [9] National Research Institute for Earth Science and Disaster Resilience (2019a): Earthquake Mechanism Information. <http://www.fnet.bosai.go.jp/event/joho.php?LANG=en>.
- [10] Kagan YY (1991): 3-D rotation of double-couple earthquake sources. *Geophysical Journal International*, **106**, 709-716.
- [11] Morikawa N, Fujiwara H (2013): A new ground motion prediction equation for Japan applicable up to M9 mega-earthquake. *Journal of Disaster Research*, **8**, 878-888.
- [12] Zhao JX, Liang FJ, Xing H, Zhu M, Hou R, Zhang Y, Lan X, Rhoades DA, Irikura K, Fukushima Y, Somerville PG (2016): Ground-motion prediction equations for subduction interface earthquakes in Japan using site class and simple geometric attenuation functions. *Bulletin of the Seismological Society of America*, **106**, 1518-1534.
- [13] Zhao JX, Jiang P, Shi H, Xing H, Huang H, Zhang Y, Yu P, Lan X, Rhoades DA, Somerville PG, Irikura K, Fukushima Y (2016): Ground-motion prediction equations for subduction slab earthquakes in Japan using site class and simple geometric attenuation functions. *Bulletin of the Seismological Society of America*, **106**, 1535-1551.
- [14] Zhao JX, Zhou S, Zhou J, Zhao C, Zhang H, Zhang Y, Gao P, Lan X, Rhoades DA, Fukushima Y, Somerville PG, Irikura K (2016): Ground-motion prediction equations for shallow crustal and upper-mantle earthquakes in Japan using site class and simple geometric attenuation functions. *Bulletin of the Seismological Society of America*, **106**, 1552-1569.
- [15] Goda K, Atkinson GM (2009): Probabilistic characterization of spatially correlated response spectra for earthquakes in Japan. *Bulletin of the Seismological Society of America*, **99**, 3003-3020.
- [16] Earthquake Research Committee, Headquarters for Earthquake Research Promotion (2018): National Seismic Hazard Maps for Japan (2018). https://www.jishin.go.jp/evaluation/seismic_hazard_map/shm_report/shm_report_2018/ (in Japanese).
- [17] National Research Institute for Earth Science and Disaster Resilience (2019b): Japan Seismic Hazard Information Station. <http://www.j-shis.bosai.go.jp/en/>.